Chem. Res. Chin. Univ., 2018, 34(2), 235—240 doi: 10.1007/s40242-018-7340-x

First-principles Study of Mechanical and Electronic Properties of Co-Sn Intermetallics for Lithium Ion Battery Anode

DONG Wei[1,2,3], SHEN Ding[1*], YANG Shaobin[1*], LIANG Bing[3], WANG Xuelei[1], LIU Yue[1] and LI Sinan[4]

1. College of Material Science and Engineering, Liaoning Technical University, Fuxin 123000, P. R. China;
2. Research Center of Coal Resources Safe Mining and Clean Utilization, Liaoning Technical University, Fuxin 123000, P. R. China;
3. College of Mechanics and Engineering, Liaoning Technical University, Fuxin 123000, P. R. China;
4. College of Mining, Liaoning Technical University, Fuxin 123000, P. R. China

Abstract The equilibrium structures, formation energy, mechanical properties and electronic properties of Co-Sn intermetallics have been systemically studied by first-principles study. The results show that the CoSn phase is more thermodynamically stable than any other stoichiometry of Co-Sn intermetallics. With the increasing of Co content in Co-Sn intermetallics, the mechanical properties change into brittle behavior from ductility character. Adding proper amount of Co to Co-Sn intermetallics can improve the cycle performance for lithium ion battery anode. However, high Co content will lead to a poor cycle performance for Co-Sn intermetallics.

Keywords Co-Sn intermetallic; Mechanical property; Electronic property; First-principle; Lithium ion battery

1 Introduction

Lithium-ion batteries(LIBs) have been widely employed for the applications in portable electronics and increasingly in electric vehicles as energy resources, because of its outstanding energy capacity, high power density and long cycle life. Graphite is one of the most commercially successful anode materials with the theoretical capacity of 372 mA h/g. However, its capacity has gradually failed to meet the growing needs of people. Therefore, substantial efforts have been focused on discovering new materials with high capacity to further improve the overall performance of LIB.

Among the possible anode material candidates, intermetallic compounds, including many compounds with Sn, have been discussed extensively, because of its higher theoretical capacity(994 mA h/g), easier for prepared and cheaper. Typically, the Co-Sn intermetallics and Co-Sn based composites have high lithium ion storage property, with smaller volume change than other Sn intermetallics during charge-discharge cycling. Jiang *et al*.[1] fabricated the hollow Co-Sn nanospheres by galvanic replacement reaction, which exhibited a good reversible capacity of 502 mA h/g at a current density of 100 mA/g and a coulomb efficiency over 99% after 100 cycles. Meng *et al*.[2] and Pang *et al*.[3] prepared Co-Sn based compounds with relatively excellent lithium ion storage property. Li *et al*.[4] found that the solid electrolyte interphase(SEI) layer of Sn-Co alloy was formed by reductive decomposition of electrolyte during the first cycle and the layer was constituted of a mixture of Li_2CO_3, $ROCO_2Li$, lithium oxalates, and/or ROLi by means of XPS and SIMS. Xiao *et al*.[5] synthesized a novel Co-Sn nanoalloy embedded in porous N-doped carbon and found the composite exhibited a high capacity of 945 mA h/g, and 86.6% capacity retention after 100 cycles at 100 mA/g as well as an excellent rate capacity. Co-Sn intermetallics and Co-Sn composites have also been applied in other fields, such as sodium ion battery[6,7].

However, the Co atoms in Co-Sn intermetallics or Co-Sn based composites act as inert element, avoiding the volume changes in the cycling and improving the structure stability at the cost of decreasing the overall specific capacity. Until now, the influence of the atomic ratio of Co to Sn on the properties of Co-Sn intermetallics itself has not been thoroughly investigated yet. The workload of using only experimental research will be great and waste a lot of time and money. Therefore, the theoretical calculations become more and more important. In many calculation methods, the first-principle calculations have made an impact on the understanding and design of lithium-ion battery materials, which is desired to avoid complex experiment and consume time. The mechanical properties of Co-Sn intermetallics could be obtained by the first-principle calculations, such as elastic constants, bulk module, Young's and shear moduli and Poisson's ratio, which are important factors of structure stability during charge-discharge cycling. Zhang *et al*.[8] calculated the relationship between volume changes and elastic-strain energies of Li-Sn alloy. Sosa-Hernández *et al*.[9] investigated the electronic properties and elastic properties of

*Corresponding authors. E-mail: yangshaobin@lntu.edu.cn; shending028@163.com

Received November 3, 2017; accepted December 13, 2017.

Supported by the National Natural Science Foundation of China(Nos.51274119, 51774175) and the Open Projects of Research Center of Coal Resources Safe Mining and Clean Utilization, Liaoning Province, China(No. LNTU16KF15).

Co_xSn_y clusters with $x+y\leqslant 5$ atoms. However, up to now, only limited information is available about the electronic and elastic properties of Co-Sn intermetallics.

In order to obtain Co-Sn intermetallic with excellent properties, the effect of different atomic ratios(Co to Sn) on the equilibrium structures, the formation energy and the electronic properties of Co-Sn intermetallic was investigated. The influence of atomic ratio(Co and Sn) on mechanical properties was mainly concerned. The mechanical properties of the Co-Sn intermetallic can reflect the structural stability of Co-Sn intermetallic to a certain extent in the cycling process of lithium ion battery, which would provide reference for further research.

2 Computational Method

The equilibrium structure, formation energy, electronic properties and mechanical properties, including the elastic constants, the bulk module and the Young's and shear moduli of Co-Sn intermetallics($CoSn_5$, $CoSn_2$ and CoSn phase) with high tin content were investigated using density functional theory calculations, as implemented in the Cambridge Serial Total Energy Package code(CASTEP)[10]. The electron-ion interactions were described through ultrasoft pseudopotentials[11] and the exchange correlation functional was constructed by the generalized gradient approximation(GGA) proposed by Perdew-Burke-Ernzerhof(PBE)[12].

The cutoff energies for the plane wave expansion of the electronic wave function were 500 eV for Co-Sn intermetallics. All atoms were fully relaxed using the conjugate gradient method until the forces were smaller than 1×10^{-3} eV/nm and the energy convergence criterion was smaller than 5×10^{-6} eV/atom. The Brillouin zone was sampled with the Monkhorst-Pack scheme[13]. For geometry optimization, the *k*-meshes considered were 8×8×8 for $CoSn_5$, 8×14×10 for $CoSn_2$ and 10×10×12 for CoSn, respectively. In the calculations, $3d^84s^1$ of Co and $5s^25p^2$ of Sn were treated as valance electron configurations and the spin-polarized approximation was used due to the ferromagnetic nature of Co atoms.

The formation energy[14,15] of Co-Sn intermetallics at 0 °C can be evaluated relative to the composition-averaged energies of the pure elements in their equilibrium crystal structures:

$$\Delta E_f(Co_mSn_n)=[E(Co_mSn_n)-mE(Co)-nE(Sn)]/(m+n) \quad (1)$$

where $\Delta E_f(Co_mSn_n)$ is the atomic formation energy of a Co_mSn_n intermetallic compound, $E(Co_mSn_n)$ is the total energy of Co_mSn_n intermetallics, E(Co) is the total energy for a Co atom in the close-packed hexagonal(*hcp*) Co metal with equilibrium lattice parameters and E(Sn) is the total energy for an Sn atom in the *β*-Sn metal with equilibrium lattice parameters.

The mechanical properties were calculated by a stress(σ)-strain(ε) approach based on the generalized Hooke's law. Thus, a proportional elastic constant C_{ij}(GPa) could be written as:

$$\sigma_i=\sum_{j=1}^{6}C_{ij}\varepsilon_{ij} \quad (2)$$

The elastic compliance matrices S_{ij} equal to C_{ij}^{-1}. In order to obtain each independent elastic constant, an appropriate number of strain patterns were imposed on crystal cell with a maximum strain value of 0.006 in the current calculations. For polycrystalline crystal, the bulk modulus(B, GPa), shear modulus(G, GPa) and Young's modulus(E, GPa) could be estimated generally with the Voigt method[16] and the Reuss method[17] from independent single-crystal elastic constants. They are given by:

$$B_V=[C_{11}+C_{22}+C_{33}+2(C_{12}+C_{13}+C_{23})]/9 \quad (3)$$

$$B_R=1/[S_{11}+S_{22}+S_{33}+2(S_{12}+S_{13}+S_{23})] \quad (4)$$

$$G_V=\{C_{11}+C_{22}+C_{33}-[C_{12}+C_{13}+C_{23}+3(C_{44}+C_{55}+C_{66})]\}/15 \quad (5)$$

$$G_R=15/[4(S_{11}+S_{22}+S_{33})-4(S_{12}+S_{13}+S_{23})+3(S_{44}+S_{55}+S_{66})] \quad (6)$$

where the subscripts V and R indicate the Voigt and Reuss averages, respectively. The Hill scheme is the arithmetic average values of the Voigt and the Reuss schemes[18], which is considered as the best estimate of the theoretical polycrystalline elastic modulus, and it can be expressed as:

$$B_H=(B_V+B_R)/2 \quad (7)$$

$$G_H=(G_V+G_R)/2 \quad (8)$$

Then, the Young's modulus(E) can be calculated from the values of elastic modulus with the relationships[19]:

$$E=9BG/(G+3B) \quad (9)$$

3 Results and Discussion

3.1 Structural Properties and Formation Energy

The Co-Sn intermetallics with high tin content have some intermediate phases, $CoSn_5$, $CoSn_2$ and CoSn, according to the Co-Sn equilibrium phase diagram[20] and other literature[21], and the crystal structures of those phases are shown in Fig.1. To determine the ground state properties of these intermetallics, the lattice constants, the positions of the internal atoms and the total energies of these Co-Sn intermediate phases together with *ε*-Co and *β*-Sn pure metals obtained from the DFT calculations and from the experiments[22—27] are displayed in Table 1. It is seen that the calculated structure parameters are in good agreement with the experimental results. The deviations between the calculated lattice constants and the experimental

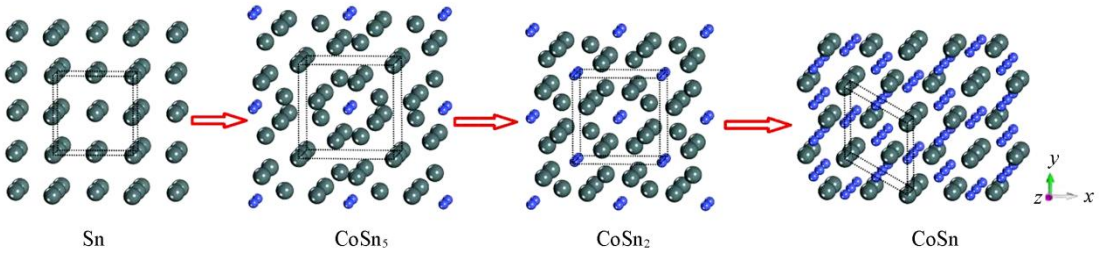

Fig.1 Crystal structures of *β*-Sn pure metals and Co-Sn intermetallics

Gray ball represents Sn atom, and blue ball represents Co atom.

Table 1 Lattice constants and total energies of these Co-Sn intermetallics together with *ε*-Co and *β*-Sn pure metals obtained from the experiments and from the DFT calculations

Structure	Space group	Atomic coordinate	*a*/nm	*b*/nm	*c*/nm	Cell volume/nm^3	Literature
β-Sn	*I*41/*amd*(141)	Sn(0, 0, 0)	0.5833	0.5833	0.3182	0.1083	Exp[22]
			0.5950	0.5950	0.3210	——	GGA[23]
			0.5967	0.5967	0.3169	0.1129	This work
$CoSn_5$	*P*4/*mcc*(124)	Co(1/2, 1/2, 1/4)	0.6933	0.6933	0.5792	——	Exp[21]
		Sn1(0, 0, 1/2)	0.7052	0.7052	0.5881	0.2924	GGA[24]
		Sn2(0.1914, 0.6101, 1/2)	0.6933	0.6933	0.5792	0.2784	This work
$CoSn_2$	*I*4/*mcm*(140)	Co(0, 0, 1/2)	0.6363	0.6363	0.5456	0.2209	Exp[25]
		Sn1(0.1649, 0.6649, 1/2)	0.6402	0.6402	0.5478	0.2245	This work
CoSn	*P*6/*mmm*(191)	Co(1/2, 0, 0)	0.5279	0.5279	0.4260	0.1028	Exp[26]
		Sn1(0, 0, 0)	0.5317	0.5317	0.4269	0.1045	This work
ε-Co	*P*63/*mmc*(194)	Sn2(1/3, 2/3, 1/2)	0.2505	0.2505	0.4089	0.0222	Exp[27]
		Co(1/3, 2/3, 1/4)	0.2509	0.2509	0.4072	0.0223	This work

results are slightly less than *ca.* 2%, which demonstrates that the computational methodology implemented in this work is suitable and the calculation results are reliable.

In order to deeply understand the difficulty of Co-Sn intermetallics formation, the formation energies of $CoSn_5$, $CoSn_2$ and CoSn obtained from the DFT calculations are shown in Fig.2 together with experimental data and the results of previous theoretical calculation. Here, the formation energies of

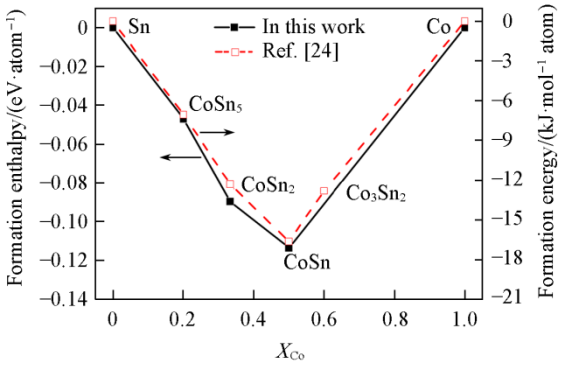

Fig.2 Calculated enthalpy of formation of Co-Sn intermetallic compound comparing with different work

$CoSn_5$, $CoSn_2$ and CoSn are –0.0471, –0.0896 and –0.1135 eV/atom, respectively. It can be seen that the tendency of the formation energy agrees well with the experimental and previous theoretical values[22—27]. In the Co-Sn binary system,CoSn phase possesses the smallest formation enthalpy, implying that the CoSn phase is more thermodynamically stable than any other stoichiometry of Co-Sn intermetallics.

3.2 Elastic Properties

The calculated independent C_{ij} values of single-crystal for the Co-Sn intermetallics are summarized in Table 2. As for the mechanical stability of a structure, these independent elastic constants should satisfy the well-known Born-Huang stability criteria[28].

For tetragonal system:

$$C_{11}>0,\ C_{33}>0,\ C_{44}>0,\ C_{66}>0,\ (C_{11}-C_{12})>0,$$
$$(C_{11}+C_{33}-2C_{13})>0,\ 2(C_{11}+C_{12})+C_{33}+4C_{13}>0$$

For hexagonal system:

$$C_{11}>0;\ C_{44}>0;\ C_{11}-C_{22}>0;\ (C_{11}-C_{12}-C_{33})>2C_{13}^2$$

The values of calculated elastic constants of Co-Sn intermetallics tabulated in Table 2 satisfy the above corresponding criteria, thereby indicating that all the Co-Sn intermetallics have mechanically stable structures at 0 Pa. In the elastic constant, C_{11} and C_{33} characterize the directional resistance to linear compression along the *x*-axis and the *z*-axis, respectively. It is seen that C_{11} is bigger than C_{33} for $CoSn_5$ and $CoSn_2$, indicating that the incompressible behavior along the *x*-axis is stronger than that of the *z*-axis. A similar trend also exists in $FeSn_2$[29]. However, an opposite trend is observed ($C_{11}<C_{33}$) in CoSn, suggesting that the incompressible behavior along *z*-axis is stronger than that along *x*-axis for CoSn.

In order to understand the elastic properties of polycrystalline Co-Sn intermetallics, the values for bulk modulus(*B*), shear modulus(*G*) and Young's modulus(*E*) of polycrystalline material using the Voigt and Reuss methods have been calculated and shown in Table 3. From the calculation results, the realistic estimates values for *B*, *G* and *E* of the polycrystalline Co-Sn intermetallics using the Hill methods are shown in Fig.3. It is clear from Fig.3 that the bulk modulus, shear modulus and Young's modulus of Co-Sn intermetallics increase with the increasing of Co concentration. The bulk modulus of $CoSn_5$(59.8 GPa) is much smaller than that of other intermetallics, implying that $CoSn_5$ has high compressibility, which may be due to the small amount of Co in the Co-Sn intermetallic.

The quotient of shear modulus to bulk modulus(*G*/*B*) can be considered as an indication of the extent of fracture range in metals. A low and a high value of *G*/*B* are associated with ductility and brittleness, respectively. From the calculations, the

Table 2 Elastic constants(C_{ij}) of single crystal Co-Sn intermetallic compound obtained from DFT

Phase	C_{11}/GPa	C_{22}/GPa	C_{33}/GPa	C_{44}/GPa	C_{55}/GPa	C_{66}/GPa	C_{12}/GPa	C_{13}/GPa	C_{23}/GPa
β-Sn	71.86	75.80	95.80	21.74	21.18	14.85	42.81	28.80	28.62
$CoSn_5$	100.22	99.21	96.36	17.06	17.77	34.93	49.12	36.96	35.98
$CoSn_2$	212.89	213.17	197.95	47.71	47.38	67.85	51.08	61.33	61.17
CoSn	231.32	230.87	265.69	70.53	70.52	67.49	95.19	66.11	66.41
ε-Co	387.74	393.44	427.59	103.23	112.44	112.44	163.67	114.34	114.38

Table 3 Bulk modulus(*B*), shear modulus(*G*), Young's modulus(*E*) and Poisson's ratio(*v*) of Co-Sn intermetallic compound obtained using Reuss(R) and Voigt(V) methods

Phase	B_V/GPa	B_R/GPa	G_V/GPa	G_R/GPa	E_V/GPa	E_R/GPa	v_V/GPa	v_R/GPa
β-Sn	49.33	49.23	21.10	19.51	55.40	51.71	0.31	0.32
$CoSn_5$	59.99	59.61	25.53	23.68	67.08	62.00	0.31	0.32
$CoSn_2$	108.66	108.63	59.98	57.05	151.98	145.64	0.27	0.28
CoSn	129.68	129.65	73.68	72.09	185.85	182.45	0.26	0.27
ε-Co	221.59	221.44	118.40	115.47	301.49	295.12	0.27	0.28

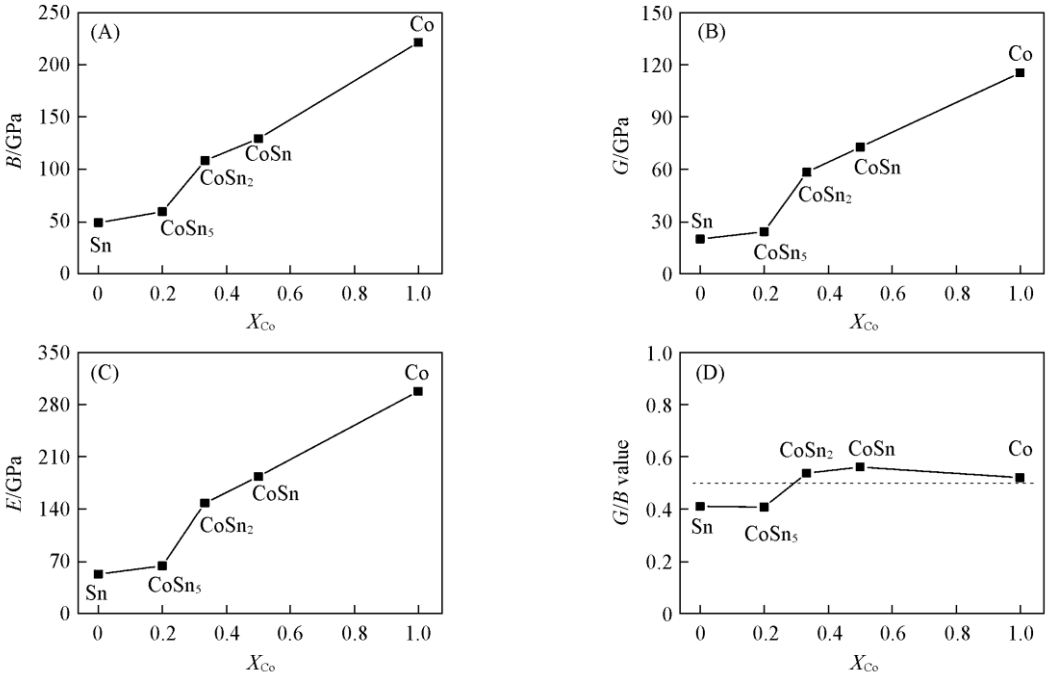

Fig.3 Bulk modulus(*B*)(A), shear modulus(*G*)(B), Young's modulus(*E*)(C) and *G*/*B* values(D) of Co-Sn intermetallic compound obtained using Hill method

G/*B* values are 0.412, 0.409 for Sn and $CoSn_5$, respectively, indicating a ductility character. The *G*/*B* values are 0.539, 0.562 and 0.521 for $CoSn_2$, CoSn and Co, respectively, suggesting a tendency to change into brittle behavior.

3.3 Nature of Bonding

For more important information about atomic-level origins of the elastic properties in Co-Sn intermetallic compound upon increasing Co concentration, the difference charge density distributions including atomic Mulliken population for $CoSn_5$, $CoSn_2$ and CoSn compounds were simulated and are represented in Fig.4.

As seen from Fig.4, the electronic charge distribution for *β*-Sn and *ε*-Co is markedly different. The electronic orbitals of each Sn atom overlap with those of the six neighboring Sn atoms, resulting in significant sharing of the electronic charge, showing a weakly covalent and directional character for the Sn—Sn bond. In contrast, the electrons of each Co atom are shared by the twelve nearest neighboring Co atoms. Meanwhile, the Sn—Sn bond length is bigger compared to the Co—Co bond(0.455 nm *vs*. 0.245 nm). Thus, the Sn—Sn bonds are not expected to be stiffer than the Co—Co bonds, which are reflected in different value between their elastic modulus as shown in Fig.4. For Co-Sn intermetallic compound, the average number of Co-Sn bonds for every Sn atom further increases to one(in $CoSn_5$), four(in $CoSn_2$) and lastly to six(in CoSn). Every Sn atom is almost surrounded by Co atoms in every direction and space, resulting in an elastic modulus similar to that of pure Co.

From atomic Mulliken population in Fig.4, it can also be known that Sn atom has a net charge of approximately from +0.12 to +0.20 and Co atoms take up −0.24 to −0.07 electrons with the increase of Co concentration. Sn donates parts of its electrons to Co atoms the nearest to a Sn atom and Co atoms typically have parts of net charge. The charge state of Sn changes depending on the amount of Co neighboring atoms and the nature of Co-Sn bond changes from metallic to partly ionic in high Co concentration compared to the crystalline *β*-Sn. Therefore, the tendency to change into brittle behavior of the Co-Sn intermetallics is consistent with the increase in the relative population of ionic bonds of the intermediate states. For Co-Sn alloy, the negative electrode materials for lithium ion batteries, adding inert element Co can improve the cycle performance, but high cobalt concentration can lead to brittleness. Therefore, adding proper amount of Co to Co-Sn intermetallics is beneficial to improve the cycle performance. The total density of states(DOSs) and partial density of states for $CoSn_5$, $CoSn_2$ and CoSn compounds as well as Sn and Co obtained from the DFT calculations are depicted in Fig.5. The Fermi level(E_F) is set to 0 eV and marked by dashed

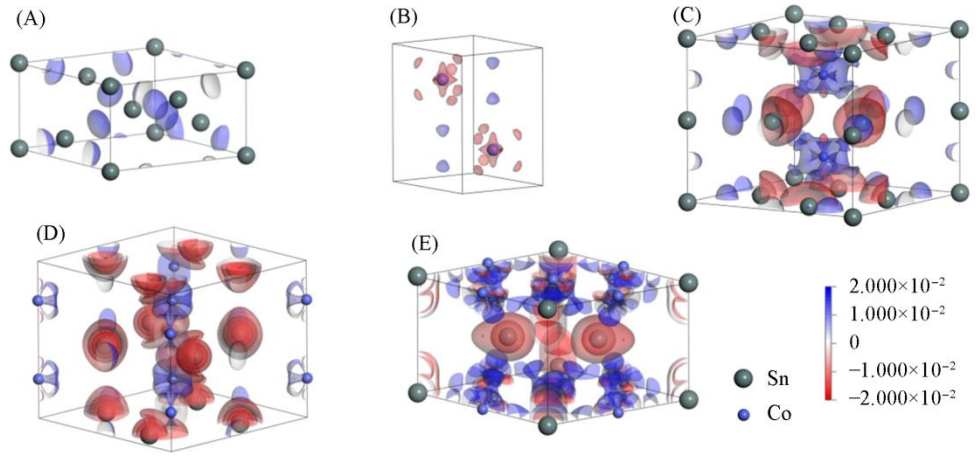

Fig.4 Charge density differences of pure Sn(A), pure Co(B), $CoSn_5$(C), $CoSn_2$(D) and CoSn(E)

lines in Fig.5. It is obvious that the orbits of different atoms contribute to the main peak of DOS and all Co-Sn intermetallics are metallic because of the finite DOS at the Fermi level. For $CoSn_5$ compounds, the sum of DOS in the zone from –11.0 eV to about –5.5 eV is mainly contributed by the Sn-*s*, from about –5.5 eV up to the Fermi level is mainly contributed by the Sn-*p* and Co-*d*, and from Fermi level to 5 eV is dominantly contributed by the Sn-*p*. The strong hybridization of Sn-*p* and Co-*d* states can be observed in the zone. And this dominant bonding mechanism of the hybridization has also been similarly found in the Ni-Sn system by Li *et al*.[30].

For the Co_2Sn and CoSn compounds, the DOS distributions are similar to each other in the whole energy range. However, the width of this band near the Fermi energy increases with the increasing of Co concentration, indicating that the contributions from Co-*d* states become more obvious and the peaks intensity increases slightly. The ε-Co itself has an outer electronic configuration of $3d^74s^2$, and the Co-*d* state plays a significant role during shearing because the Co-*s* state and the Co-*p* state are relatively weak in the entire region.

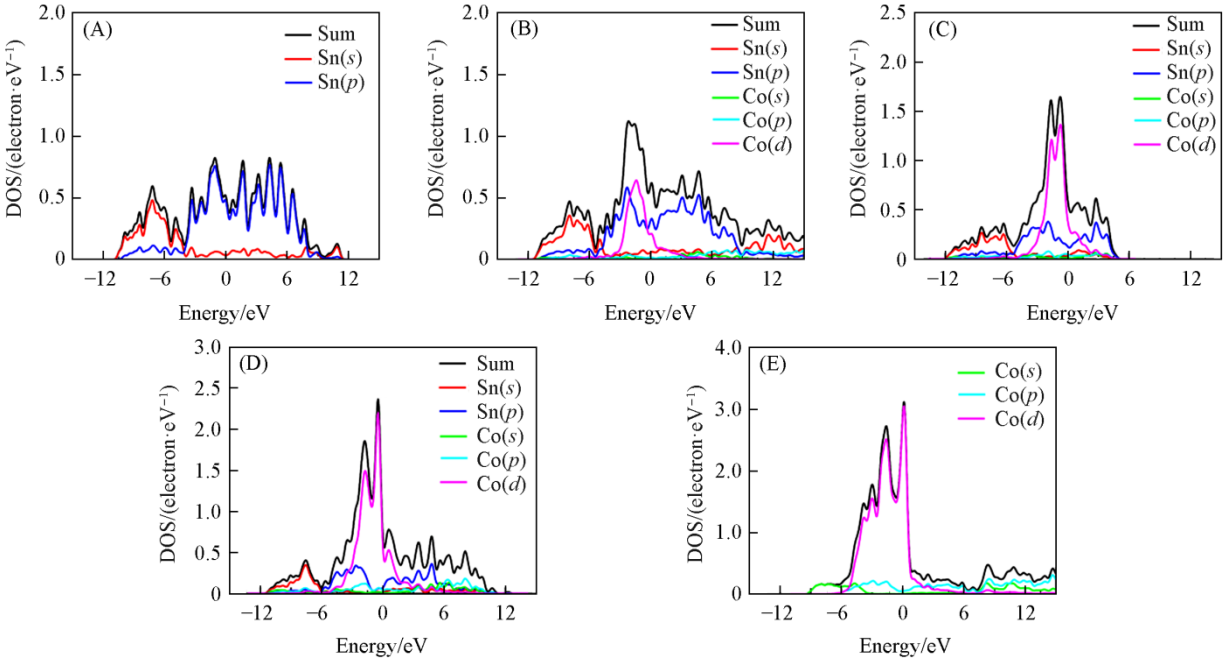

Fig.5 Total and partial density of states for the Co-Sn intermetallics of Sn(A), Sn_5Co(B), Sn_2Co(C), SnCo(D) and Co(E)

4 Conclusions

The equilibrium structures, formation energy, mechanical properties and electronic properties of Co-Sn intermetallics were systemically studied *via* the first-principles study. The results showed that the CoSn phase was more thermodynamically stable than any other stoichiometry of Co-Sn intermetallics. With the increasing of Co content in Co-Sn intermetallics, the mechanical properties changed into brittle behavior from ductility character. The increase of brittleness easily led to the Co-Sn alloy structure being more easily damaged due to the volume expansion during charging and discharging. Therefore, the cycling performance of the alloy with high content of Co is not always optimal, which is different from the conventional knowledge. The rational control of the atomic ratio of Co to Sn is very important and necessary for improving the

electrochemical performance of Co-Sn intermetallics.

References

[1] Jiang A. N., Fan X., Zhu J., Ma D. Q., Xu X. H., *Ionics*, **2015**, *21*(8), 2137

[2] Meng H. W., Yang H. Y., Yu X. H., Dou P., Ma D. Q., Xu X. H., *RSC Advances*, **2015**, *5*(116), 95488

[3] Pang X. J., Tan C. H., Dai X. H., Wang X., Qi G. W., Zhang S. Y., *J. Appl. Electrochem.*, **2015**, *45*(2), 115

[4] Li J. T., Swiatowska J., Seyeux A., Huang L., Maurice V., Sun S. G., Marcus P., *J. Power Sources*, **2010**, *195*(24), 8251

[5] Xiao S., Song H., Li A., Chen X. H., Zhou J. S., Ma Z. K., *J. Mater. Chem. A*, **2017**, *5*(12), 5873

[6] Yui Y., Ono Y., Hayashi M., Nemoto Y., Hayashi K., Asakura K., Kitabayashi H., *J. Electrochem. Soc.*, **2015**, *162*(2), A3098

[7] Yui Y. H., Hayashi M., Hayashi K., Nakamura J., *Solid State Ionics*, **2016**, *288*, 219

[8] Zhang F., Wang J. C., Liu S. H., Du Y., *J. Power Sources*, **2016**, *330*, 111

[9] Sosa-Hernández E. M., Montejano-Carrizales J. M., Alvarado-Leyva P. G., *J. Alloys Compounds*, **2015**, *632*, 772

[10] Clark S. J., Segall M. D., Pickard C. J., Hasnip P. J., Probert M. I., Refson K., Payne M. C., *Zeitschrift für Kristallographie-Crystalline Materials*, **2005**, *220*(5/6), 567

[11] Vanderbilt D., *Phys. Rev. B*, **1990**, *41*(11), 7892

[12] Perdew J. P., Burke K., Ernzerhof M., *Phys. Rev. Lett.*, **1996**, *77*(18), 3865

[13] Monkhorst H. J., Pack J. D., *Phys. Rev. B*, **1976**, *13*(12), 5188

[14] Colinet C., Tedenac J. C., Fries S. G., *Calphad*, **2009**, *33*(1), 250

[15] Chen J., Lai Y. S., *Microelectronics Reliability*, **2009**, *49*(3), 264

[16] Voigt W., *Annalen der Physik*, **1889**, *274*(12), 573

[17] Reuss A., *Z. Angew. Math. Mech.,* **1929**, *9*, 49

[18] Hill R., *Proc. Phys. Soc.: Section A*, **1952**, *65*(5), 349

[19] Simmons G., Wang H. B., *Single Crystal Elastic Constants & Calculated Aggregate Properties,* **1971**, 34

[20] Ishida K., Nishizawa T., *J. Phase Equilibria*, **1991**, *12*(1), 88

[21] Wang X. L., Chen H., Bai J., Han W. Q., *J. Phys. Chem. Lett.*, **2012**, *3*(11), 1488

[22] Liu M, Liu L. G., *High Temperatures-High Pressures*, **1986**, *18*, 79

[23] Mortazavi M., Deng J. K., Shenoy V. B., Medhekar N. V., *J. Power Sources*, **2013**, *225*, 207

[24] Sun W. M., Zhang L., Liu J., Wang H., Bu Y. X., *Computational Materials Science*, **2016**, *111*, 175

[25] Havinga E. E., *J. Less Common Metals*, **1972**, *27*(2), 187

[26] Larsson A. K., Haeberlein M., Lidin S., Schwarz U., *J. Alloy. Comp.*, **1996**, *240*(1/2), 79

[27] Owen E. A., Madoc J. D., *Proc. Phys. Soc. B*, **1954**, *67*(6), 456

[28] Max B., Kun H., *Dynamical Theory of Crystal Lattices*, Clarendon, Oxford, **1956**, 132

[29] Wang X. L., Feygenson M., Chen H., Lin C. H., Ku W., Bai J., Han W. Q., *J. Am. Chem. Soc.*, **2011**, *133*(29), 1121

[30] Li L. H., Wang W. L., Wei B., *Comput. Mater. Sci.*, **2015**, *99*, 274